Polymer Journal (2017) 49, 633–637

www.nature.com/pj

NOTE

Scattering function of semi-rigid cyclic polymers analyzed in terms of worm-like rings: cyclic amylose tris(phenylcarbamate) and cyclic amylose tris(*n*-butylcarbamate)

Akiyuki Ryoki[1], Daichi Ida[2] and Ken Terao[1]

Recently reported data of the particle scattering function *P*(*q*) with the magnitude *q* of the scattering vector for rigid cyclic amylose tris(phenylcarbamate) (cATPC) and cyclic amylose tris(*n*-butylcarbamate) (cATBC) in different solvents were analyzed in terms of a novel simulation method based on the Kratky–Porod worm-like chain model. Although similar worm-like chain parameters were evaluated for both relatively flexible cyclic chains and the corresponding linear polymers, an appreciable decrease in the chain stiffness and slight extension of the local helical structure were found for cyclic chains with a higher chain stiffness. The difference in the worm-like chain parameters between the cyclic and linear chains cannot be realized in the previously reported molar mass dependence of the radius of gyration. This suggests that analyses of *P*(*q*) are decisively important to understand the conformational properties of rigid and/or semi-flexible cyclic chains in solution if the molar mass range of the cyclic polymer samples is limited.
Polymer Journal (2017) **49,** 633–637; doi:10.1038/pj.2017.27; published online 10 May 2017

The local conformation of ring or cyclic chains is substantially the same as that of their linear analogs if the chain length is sufficiently longer than the Kuhn segment length λ^{-1}, which is the chain stiffness parameter of the Kratky–Porod worm-like chain.[1] The discrepancy between cyclic and linear polymers may become significant upon shortening or stiffening the main chain because the difference in the curvature distribution becomes prominent owing to the topological constraint. Little is known, however, about the chain stiffness (or length) -dependent local conformational change, except for the case of the super-helical structure of cyclic DNA,[2] although abundant studies have examined the physical properties of rather flexible cyclic polymers including polystyrene,[3–9] polydimethylsiloxane[10,11] and polysaccharides.[12–15] This is likely because cyclic polymers are synthesized by end-linking or ring expansion methods. A variety of novel cyclic polymers have recently been reported not only for fundamental synthetic studies, but also for building blocks of higher order structures consisting of amphiphilic block copolymers.[16–19] Considering that dense macrocyclic comb polymers that should have relatively stiff main chains form tube-like complexes,[20] the chain stiffness effect on the dimensional properties and intermolecular interactions should be an important topic.

Semi-flexible and rigid cyclic polymers were recently obtained by means of 'stiffening' the main chain of rather flexible cyclic chains. Cyclic amylose tris(phenylcarbamate) (cATPC)[21] and cyclic amylose tris(*n*-butylcarbamate) (cATBC)[22] prepared from enzymatically synthesized cyclic amylose[23] behave as semi-flexible and/or rigid cyclic macromolecules in solution. The molar mass dependence of the mean square radius of gyration $\langle S^2 \rangle$ for cATPC and cATBC in various solvents is fairly explained by current theories for the cyclic worm-like chain[24] with the parameters, λ^{-1} and the helix pitch (or helix rise) h per unit chain length, determined for the corresponding linear chains.[21,22] The experimental values for cATPC in some ketones and esters are, however, appreciably smaller than the theoretical values calculated with the parameters so determined.[25] This suggests that both the local helical structure and the chain stiffness depend on the molar mass of the cyclic polymer chains. Although the particle scattering function $P(q)$ was determined as a function of the magnitude q of the scattering vector for the two cyclic polymers in different solvents,[21,22] appropriate theories or simulation data were not yet available for semi-rigid cyclic chains. Recently, Ida and colleagues[26,27] calculated $P(q)$ for worm-like rings with a variety of reduced chain lengths, that is, the ratio of the contour length L to λ^{-1} or the Kuhn segment number N_K, allowing us to compare them with experimental $P(q)$ data. We thus reanalyzed the previously published $P(q)$ data to discuss the difference between the molecular structures of linear and cyclic amylose derivatives in solution.

[1]Department of Macromolecular Science, Graduate School of Science, Osaka University, Osaka, Japan and [2]Department of Polymer Chemistry, Graduate School of Engineering, Kyoto University, Kyoto, Japan
Correspondence: Dr K Terao, Department of Macromolecular Science, Graduate School of Science, Osaka University, 1-1 Machikaneyama-cho, Toyonaka, Osaka 560-0043, Japan.
E-mail: kterao@chem.sci.osaka-u.ac.jp
Received 1 March 2017; revised 27 March 2017; accepted 3 April 2017; published online 10 May 2017

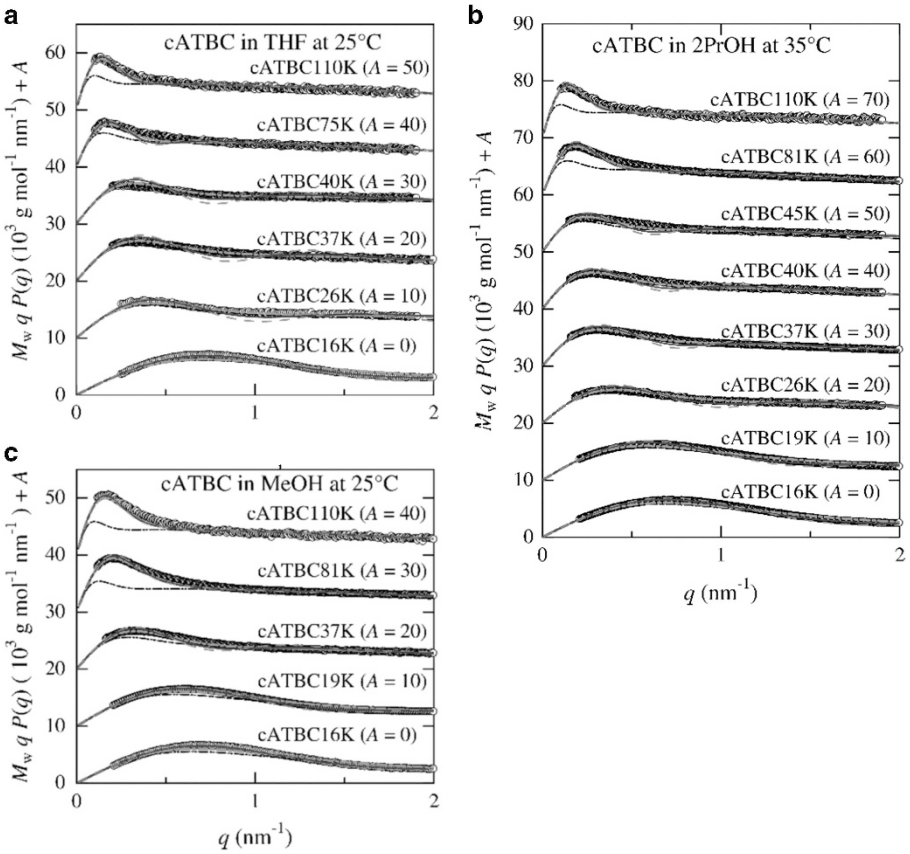

Figure 1 Comparison between the experimental $P(q)$ data[22] (unfilled circles) and the theoretical values for the indicated cATBC samples in tetrahydrofuran (THF) at 25 °C (**a**), in 2-propanol (2PrOH) at 35 °C (**b**) and in methanol (MeOH) at 25 °C (**c**). Dashed, solid and dot-dashed curves are the simulation values for the worm-like ring model with the dispersity index $Đ = 1.00$, 1.05 and 1.20, respectively. The double-dot-dashed black curve represents the theoretical values for the rigid ring ($Đ = 1.2$). The ordinate values are shifted by A for clarity. A full color version of this figure is available at *Polymer Journal* online.

The previously reported $P(q)$ data[21,22] for cATPC in 1,4-dioxane (DIOX), 2-ethoxyethanol (2EE), methyl acetate (MEA), ethyl acetate (EA), and 4-methyl-2-pentanone (MIBK) and cATBC in methanol (MeOH), 2-propanol (2PrOH), and tetrahydrofuran (THF) were determined at the BL40B2 beamline in SPring-8 and the BL-10C beamline in KEK-PF. They were obtained for five cATPC and nine cATBC samples ranging in weight-average molar mass M_w between 1.25×10^4 g mol^{-1} and 1.49×10^5 g mol^{-1} for cATPC and 1.60×10^4 g mol^{-1} and 1.11×10^5 g mol^{-1} for cATBC, corresponding to numbers of saccharide units between 24 and 290 for the former polymer, and between 35 and 240 for the latter. The dispersity index $Đ$ defined as the ratio of M_w to the number-average molar mass was estimated to be 1.05–1.23.

Monte Carlo simulations were performed using the method reported by Ida *et al.*[27,28] to calculate the particle scattering function $P_0(q)$ of worm-like rings without chain thickness as a function of N_K ($\equiv \lambda L$). A discrete worm-like chain model originally proposed by Frank-Kamenetskii *et al.*[29] was used with the bond number being 200. For each N_K, 10^5 configurations were generated to obtain an ensemble average with the appropriate monitoring steps. According to our previous study,[21,22] the chain thickness significantly affects $P(q)$ at a relatively high q range. The relationship can be considered by means of the touched bead model[30,31] as follows:

$$P(q) = 9\left(\frac{2}{qd_b}\right)^6\left(\sin\frac{qd_b}{2} - \frac{qd_b}{2}\cos\frac{qd_b}{2}\right)^2 P_0(q) \qquad (1)$$

Since actual cATPC and cATBC samples have finite molar mass distributions, the z-average particle scattering function $P_z(q)$ with a log-normal distribution was calculated numerically to compare the experimental data.

The calculated $P_z(q)$ or $P(q)$ values with the best fit parameters λ^{-1} and h for cATBC in three solvents are plotted in Figure 1. The calculated values of $P_z(q)$ with appropriate $Đ$ (1.05 (blue) and 1.20 (red)) well explain the behavior of the experimental data, while those of $P(q)$ for the monodisperse ring (green) slightly deviate downward in the middle-q range from the experimental values for the lower-M_w samples. Good agreement was observed between the simulation and experimental data for cATPC in six solvent systems (see Supplementary Figure S1 in the Supplementary Information). We note that the values of λ^{-1} may be determined without ambiguity only for the samples with high M_w, for which the theoretical values for the rigid ring calculated with the appropriate h value (black dot-dashed curves) underestimate $P(q)$ at approximately $q = 0.2$ nm^{-1}. We then adopted the λ^{-1} value determined for the samples with high M_w to calculate $P_z(q)$ or $P(q)$ for the samples with low M_w. We also note that $P_z(q)$ and $P(q)$ become insensitive to changes in λ^{-1} with decreasing M_w. The other two parameters, h and d_b, were uniquely determined for more samples, except for the two lowest M_w samples, for both cATBC and cATPC. The latter parameter d_b was consistent with those for the corresponding linear chain within ±11% if we estimate d_b for the linear polymer from the literature chain diameter d values[32–35] for the cylinder model by means

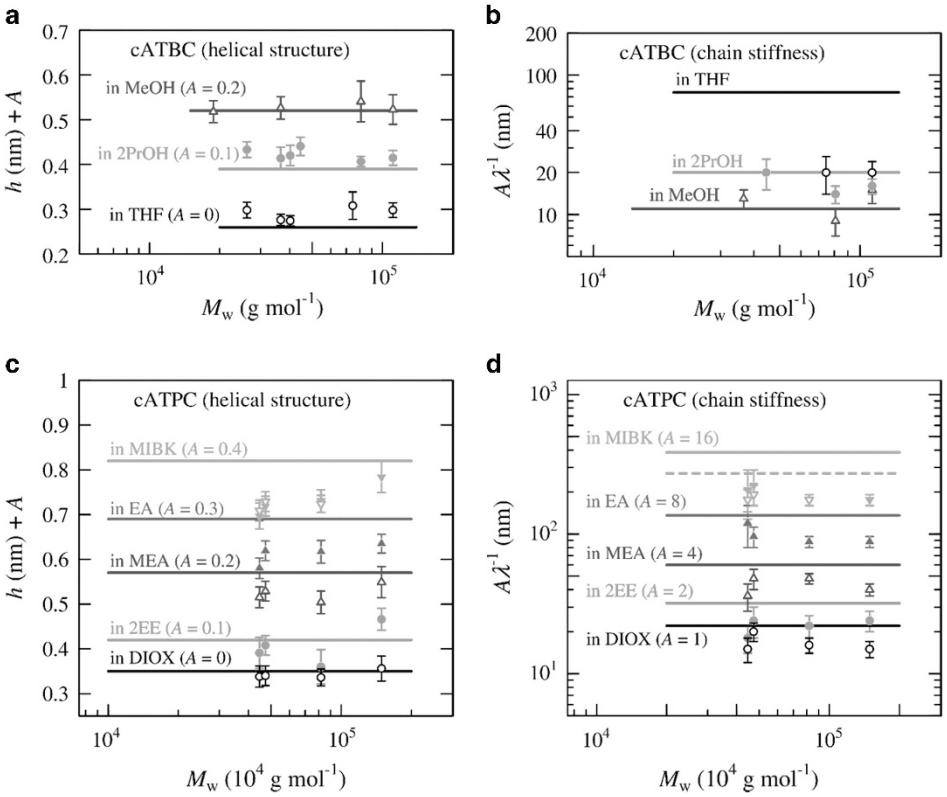

Figure 2 Weight-average molar mass M_w dependence of the worm-like chain parameters for cATBC and cATPC in solution. In (**a**, **b**), the unfilled circles, filled circles and triangles indicate the parameters for cATBC in THF at 25 °C, in 2PrOH at 33 °C and in MeOH at 25 °C, respectively. The solid lines are h or λ^{-1} for the corresponding linear chain. In (**c**, **d**), the unfilled circles, filled circles, unfilled triangles, filled triangles, unfilled inverted triangles and filled inverted triangles represent the parameters for cATPC in DIOX at 25 °C, in 2EE at 25 °C, in MEA at 25 °C, in EA at 33 °C, and in MIBK at 25 and 58 °C, respectively. The solid and dashed magenta lines in (**d**) are the λ^{-1} values for linear ATPC in MIBK at 25 and 58 °C, respectively. The ordinate values are shifted by A for clarity. A full color version of this figure is available at *Polymer Journal* online.

of the known relationship $d_b = 1.118\ d$.[36] The negligible difference between the $P(q)$ data for the discrete worm-like chain and those for the continuous rigid cyclic chain in the high q region supports that the current simulation results are substantially the same as those for the continuous chain.

The determined λ^{-1} and h values are plotted against M_w in Figure 2. The former parameter λ^{-1} for cATBC in THF is much smaller than that for the linear ATBC. This difference is clearly recognized from the fact that the calculated values of $P_z(q)$ and $P(q)$ for cATBC in THF with the parameters determined for linear ATBC ($h = 0.28$ nm and $\lambda^{-1} = 75$ nm) are appreciably smaller than the experimental values, as shown in Supplementary Figure S2 in the Supplementary Information. On the other hand, the theoretical values of $\langle S^2 \rangle$ for worm-like rings calculated from the Shimada–Yamakawa equation[24] with the parameters determined currently for cATBC ($h = 0.33$ nm and $\lambda^{-1} = 20$ nm) and those calculated using the previously estimated values ($h = 0.28$ nm and $\lambda^{-1} = 75$ nm)[22] assuming λ^{-1} for linear ATBC[18] are indistinguishable in the investigated M_w range, as shown in Supplementary Figure S3 in the Supplementary Information. This indicates that the worm-like chain parameters for this system cannot be determined only from the reported $\langle S^2 \rangle$ data. When we consider that the worm-like chain parameters of infinitely long cyclic chains should be the same as those for the corresponding linear chains, as mentioned in the 'Introduction,' it is expected that a molar mass-dependent chain stiffness could be observed in the higher molar mass range. In the case of h, its values for most cases of cyclic chains are fairly identical to

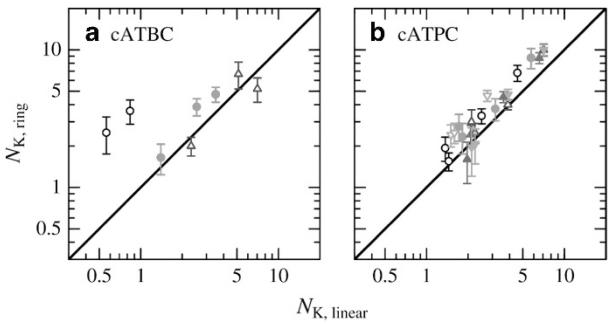

Figure 3 Double logarithmic plots of $N_{K,ring}$ vs $N_{K,linear}$ for (**a**) cATBC and (**b**) cATPC in various solvents. The symbols are the same as those used in Figure 2. The solid lines indicate $N_{K,ring} = N_{K,linear}$. A full color version of this figure is available at *Polymer Journal* online.

those of the corresponding linear chains, except for cATPC in MIBK, cATPC in EA, cATBC in THF and cATBC in 2PrOH. The former two polymer-solvent systems are rather specific because hydrogen bonding solvent molecules extend and stiffen the linear ATPC, while in the latter cases, the rigid helical main chain of ATBC in THF (or 2PrOH) is extended by the cyclization similarly to the case with bended helical springs. This local structural change also reduces the chain stiffness of the main chain of cATBC. It is, however, noted that this local structural change is insensitive to the solution infrared absorption, which reflects the intramolecular hydrogen bonds.[22]

The Kuhn segment numbers $N_{K,ring}$ for cATBC and cATPC are plotted against that for the corresponding linear chain $N_{K,linear}$ in Figure 3. Note that $N_{K,linear}$ was calculated from the worm-like chain parameters reported for the corresponding linear chain with the same M_w. This number is well-known as a universal parameter that mainly reflects the chain conformation of unperturbed linear polymer chains in solution. Interestingly, in the range of $N_{K,linear} > 1.5$, $N_{K,ring}$ is fairly close to $N_{K,linear}$, in contrast to the case of cATBC in THF in the range of $N_{K,linear} < 1$, for which λ^{-1} is clearly smaller than that of the linear ATBC (Figure 2b). The threshold value 1.0–1.5 of N_K is close to the value at which the (angle-independent) ring closure probability for the (linear) worm-like chain significantly increases.[37] It is, however, noted that $N_{K,ring}$ for ATPC in EA and MIBK is incidentally close to $N_{K,linear}$, although h and λ^{-1} for cATPC are smaller than those for linear ATPC (Figure 2c and d). As mentioned above and in previous papers,[17,38] the origin of the chain stiffness of these systems is different from that of other systems. We may thus conclude that some strain effects for cyclic chains arising from the relaxation of the internal-rotation-angle distribution in their main chain become appreciable for shorter (stiffer) cyclic chains with small N_K. In contrast, λ^{-1} for the cyclic chain is substantially the same as that for the corresponding linear chain when N_K is larger, and the local helical structure of the cyclic chain is almost identical to that of the corresponding linear chain. Although such a threshold value of N_K may depend on the polymer-solvent system and/or the origin of the chain stiffness, for example, differences in h and λ^{-1} between cyclic and linear chains were reported for ATPC in EA and MIBK (Figure 2c and d) in the range of N_K from 0.42 to 6.6,[25] such strain effects seem to make cyclic chains more flexible than linear chains as far as amylose carbamates are concerned. Unfortunately, however, it is still not clear whether rigid cyclic chains should have a smaller λ^{-1} compared to the corresponding linear chains. It is desirable to test other rigid cyclic chain systems to clarify this issue.

We reanalyzed our recently published scattering function data for cATBC in three and cATPC in five solvent systems in terms of the cyclic worm-like chain to determine the contour length per residue h and the Kuhn segment length λ^{-1} (stiffness parameter). While there was no significant molar mass dependence of the worm-like chain parameters, a clearly small λ^{-1} was estimated for cATBC in THF, even though the difference cannot be distinguishable from the radius of gyration, showing that the analysis of the particle scattering function of the cyclic chain is important to determining the chain shape of the rigid cyclic chains in solution.

CONFLICT OF INTEREST

The authors declare no conflict of interest.

ACKNOWLEDGEMENTS

We thank Professor Takenao Yoshizaki at Kyoto University and Professor Takahiro Sato at Osaka University for fruitful discussions. This work was partially supported by JSPS KAKENHI Grant nos 23750128 and 25410130. The original SAXS data were acquired at the BL40B2 beamline in SPring-8 with the approval of the Japan Synchrotron Radiation Research Institute (JASRI) (proposal no. 2010B1126, 2011A1049 and 2011B1068) and at the BL-10C beamline in KEK-PF under the approval of the Photon Factory Program Advisory Committee (proposal no. 2010G080 and 2011G557).

1 Kratky, O. & Porod, G. Rontgenuntersuchung geloster fadenmolekule. *Recl. Trav. Chim. Pays-Bas* **68**, 1106–1122 (1949).
2 Vologodskii, A. V. & Cozzarelli, N. R. Conformational and thermodynamic properties of supercoiled DNA. *Annu. Rev. Biophys. Biomol. Struct.* **23**, 609–643 (1994).
3 Roovers, J. & Toporowski, P. M. Synthesis of high molecular-weight ring polystyrenes. *Macromolecules* **16**, 843–849 (1983).
4 Ragnetti, M., Geiser, D., Hocker, H. & Oberthur, R. C. Small-angle neutron-scattering (sans) of cyclic and linear polystyrene in toluene. *Macromol. Chem. Phys.* **186**, 1701–1709 (1985).
5 Lutz, P., McKenna, G. B., Rempp, P. & Strazielle, C. Solution properties of ring-shaped polystyrenes. *Macromol. Chem. Rapid Commun.* **7**, 599–605 (1986).
6 Hadziioannou, G., Cotts, P. M., Tenbrinke, G., Han, C. C., Lutz, P., Strazielle, C., Rempp, P. & Kovacs, A. J. Thermodynamic and hydrodynamic properties of dilute-solutions of cyclic and linear polystyrenes. *Macromolecules* **20**, 493–497 (1987).
7 McKenna, G. B., Hostetter, B. J., Hadjichristidis, N., Fetters, L. J. & Plazek, D. J. A study of the linear viscoelastic properties of cyclic polystyrenes using creep and recovery measurements. *Macromolecules* **22**, 1834–1852 (1989).
8 Takano, A., Ohta, Y., Masuoka, K., Matsubara, K., Nakano, T., Hieno, A., Itakura, M., Takahashi, K., Kinugasa, S., Kawaguchi, D., Takahashi, Y. & Matsushita, Y. Radii of gyration of ring-shaped polystyrenes with high purity in dilute solutions. *Macromolecules* **45**, 369–373 (2012).
9 Gooßen, S., Brás, A. R., Pyckhout-Hintzen, W., Wischnewski, A., Richter, D., Rubinstein, M., Roovers, J., Lutz, P. J., Jeong, Y., Chang, T. & Vlassopoulos, D. Influence of the solvent quality on ring polymer dimensions. *Macromolecules* **48**, 1598–1605 (2015).
10 Dodgson, K., Sympson, D. & Semlyen, J. A. Studies of cyclic and linear poly(dimethyl siloxanes): 2. Preparative gel-permeation chromatography. *Polymer* **19**, 1285–1289 (1978).
11 Higgins, J. S., Dodgson, K. & Semlyen, J. A. Studies of cyclic and linear poly(dimethyl siloxanes). 3. Neutron-scattering measurements of the dimensions of ring and chain polymers. *Polymer* **20**, 553–558 (1979).
12 Kitamura, S., Isuda, H., Shimada, J., Takada, T., Takaha, T., Okada, S., Mimura, M. & Kajiwara, K. Conformation of cyclomaltooligosaccharide ('cycloamylose') of dp21 in aqueous solution. *Carbohydr. Res.* **304**, 303–314 (1997).
13 Shimada, J., Kaneko, H., Takada, T., Kitamura, S. & Kajiwara, K. Conformation of amylose in aqueous solution: small-angle x-ray scattering measurements and simulations. *J. Phys. Chem. B* **104**, 2136–2147 (2000).
14 Nakata, Y., Amitani, K., Norisuye, T. & Kitamura, S. Translational diffusion coefficient of cycloamylose in aqueous sodium hydroxide. *Biopolymers* **69**, 508–516 (2003).
15 Suzuki, S., Yukiyama, T., Ishikawa, A., Yuguchi, Y., Funane, K. & Kitamura, S. Conformation and physical properties of cycloisomaltooligosaccharides in aqueous solution. *Carbohydr. Polym.* **99**, 432–437 (2014).
16 Deffieux, A., & Schappacher, M. in *Polymer Science: A Comprehensive Reference*, (eds Matyjaszewski, K. & Möller, M.), 5–28 (Elsevier, Amsterdam, Netherlands, 2012).
17 Pangilinan, K. & Advincula, R. Cyclic polymers and catenanes by atom transfer radical polymerization (atrp). *Polym. Int.* **63**, 803–813 (2014).
18 Williams, R. J., Dove, A. P. & O'Reilly, R. K. Self-assembly of cyclic polymers. *Polym. Chem.* **6**, 2998–3008 (2015).
19 Yamamoto, T. & Tezuka, Y. Cyclic polymers revealing topology effects upon self-assemblies, dynamics and responses. *Soft Matter* **11**, 7458–7468 (2015).
20 Schappacher, M. & Deffieux, A. Synthesis of macrocyclic copolymer brushes and their self-assembly into supramolecular tubes. *Science* **319**, 1512–1515 (2008).
21 Terao, K., Asano, N., Kitamura, S. & Sato, T. Rigid cyclic polymer in solution: cycloamylose tris(phenylcarbamate) in 1,4-dioxane and 2-ethoxyethanol. *ACS Macro Lett.* **1**, 1291–1294 (2012).
22 Terao, K., Shigeuchi, K., Oyamada, K., Kitamura, S. & Sato, T. Solution properties of a cyclic chain having tunable chain stiffness: cyclic amylose tris(*n*-butylcarbamate) in θ and good solvents. *Macromolecules* **46**, 5355–5362 (2013).
23 Takaha, T., Yanase, M., Takata, H., Okada, S. & Smith, S. M. Potato d-enzyme catalyzes the cyclization of amylose to produce cycloamylose, a novel cyclic glucan. *J. Biol. Chem.* **271**, 2902–2908 (1996).
24 Shimada, J. & Yamakawa, H. Moments for DNA topoisomers: the helical wormlike chain. *Biopolymers* **27**, 657–673 (1988).
25 Asano, N., Kitamura, S. & Terao, K. Local conformation and intermolecular interaction of rigid ring polymers are not always the same as the linear analogue: cyclic amylose tris (phenylcarbamate) in theta solvents. *J. Phys. Chem. B* **117**, 9576–9583 (2013).
26 Tsubouchi, R., Ida, D., Yoshizaki, T. & Yamakawa, H. Scattering function of wormlike rings. *Macromolecules* **47**, 1449–1454 (2014).
27 Ida, D. Dilute solution properties of semiflexible star and ring polymers. *Polym. J.* **46**, 399–404 (2014).
28 Ida, D., Nakatomi, D. & Yoshizaki, T. A monte carlo study of the second virial coefficient of semiflexible ring polymers. *Polym. J.* **42**, 735–744 (2010).
29 Frank-Kamenetskii, M. D., Lukashin, A. V., Anshelevich, V. V. & Vologodskii, A. V. Torsional and bending rigidity of the double helix from data on small DNA rings. *J. Biomol. Struct. Dyn.* **2**, 1005–1012 (1985).
30 Burchard, W. & Kajiwara, K. The statistics of stiff chain molecules. I. The particle scattering factor. *Proc. R. Soc. Lond. Ser. A* **316**, 185–199 (1970).
31 Nagasaka, K., Yoshizaki, T., Shimada, J. & Yamakawa, H. More on the scattering function of helical wormlike chains. *Macromolecules* **24**, 924–931 (1991).
32 Terao, K., Fujii, T., Tsuda, M., Kitamura, S. & Norisuye, T. Solution properties of amylose tris(phenylcarbamate): local conformation and chain stiffness in 1,4-dioxane and 2-ethoxyethanol. *Polym. J.* **41**, 201–207 (2009).
33 Fujii, T., Terao, K., Tsuda, M., Kitamura, S. & Norisuye, T. Solvent-dependent conformation of amylose tris(phenylcarbamate) as deduced from scattering and viscosity data. *Biopolymers* **91**, 729–736 (2009).
34 Terao, K., Murashima, M., Sano, Y., Arakawa, S., Kitamura, S. & Norisuye, T. Conformational, dimensional, and hydrodynamic properties of amylose

tris(*n*-butylcarbamate) in tetrahydrofuran, methanol, and their mixtures. *Macromolecules* **43**, 1061–1068 (2010).
35 Sano, Y., Terao, K., Arakawa, S., Ohtoh, M., Kitamura, S. & Norisuye, T. Solution properties of amylose tris(*n*-butylcarbamate). Helical and global conformation in alcohols. *Polymer* **51**, 4243–4248 (2010).
36 Nakamura, Y. & Norisuye, T. Scattering function for wormlike chains with finite thickness. *J. Polym. Sci. B Polym. Phys.* **42**, 1398–1407 (2004).
37 Yamakawa, H. & Yoshizaki, T. *Helical Wormlike Chains in Polymer Solutions* 2nd edn (Springer, Heidelberg, Germany, 2016).
38 Tsuda, M., Terao, K., Nakamura, Y., Kita, Y., Kitamura, S. & Sato, T. Solution properties of amylose tris(3,5-dimethylphenylcarbamate) and amylose tris(phenylcarbamate): side group and solvent dependent chain stiffness in methyl acetate, 2-butanone, and 4-methyl-2-pentanone. *Macromolecules* **43**, 5779–5784 (2010).

Supplementary Information accompanies the paper on Polymer Journal website (http://www.nature.com/pj)